Adaptive Robust Control for Trajectory Tracking of Autonomous underwater Vehicles on Horizontal Plane

N. Zendehdel, J. Sadati[*] and A. Ranjbar N.

Faculty of Electrical & Computer Engineering, Babol Noshirvani University of Technology, Babol, Mazandaran, Iran.

Abstract
This paper addresses the trajectory tracking problem of autonomous underwater vehicles in the horizontal plane. Adaptive sliding mode control is employed in order to achieve a robust behavior against some uncertainty and ocean current disturbances, assuming that disturbance and its derivative are bounded by unknown boundary levels. The proposed approach is based upon a dual layer adaptive law, which is independent from the knowledge of disturbance boundary limit and its derivative. This approach tends to play a significant role in reducing the chattering effect that is prevalent in the conventional sliding mode controllers. To guarantee the stability of the proposed control technique, the Lyapunov theory is used. The simulation results illustrate the validity of the proposed control scheme compared to the finite-time tracking control method.

Keywords: *Autonomous Underwater Vehicle, Trajectory Tracking, Adaptive Control, Sliding Mode Control.*

1. Introduction
Submarines play an important role in underwater exploration, mapping, scientific missions, and so forth. Therefore, navigation and control systems of Autonomous Underwater Vehicles (AUVs) have gained a remarkable importance in the recent years. Since severe conditions and deep regions of oceans tend to threaten the human beings' lives, applying manned submarines is not recommended. In these situations, AUVs can be considered as a suitable alternative for manned underwater vehicles. As AUVs are unmanned vehicles without any remote control, they require autonomous motion control techniques in order to accomplish their missions. To solve this issue, various motion control approaches have been taken into account, and these techniques can be generally classified into three categories:

- Trajectory tracking control
- Path-following control
- Way-point tracking control

Trajectory tracking control is attributed to the case when a desired trajectory needs to be tracked from an initial point A to a desired point B at a desired time. In other words, the continuous sequence coincidence of each position of an AUV at any time with the desired time-parameterized trajectory is called the trajectory tracking [1]. In the path-following control, 'time' is not of concern but following the desired path is the objective [2]. The way-point tracking control refers to tracking a desired set of discrete points between the initial and the final points. In the way-point tracking control strategy, the AUV control system enforces the vehicle to find the optimized path between two desired sequential points [3]. From different viewpoints, the time-varying trajectory is more practical than the other categories, and that is why it has captured more attention than the path-following control [4]. Hence, it is addressed as the main issue in this paper.

The performance of AUVs is highly dependent on the design procedure, environmental and working conditions, uncertainties, and external disturbances. Generally, the mathematical model of AUVs is highly non-linear, becoming more complicated when the uncertainty terms and external disturbances such as ocean waves are added. To tackle this issue, many researchers have

proposed various simplified methods such as linearizing in the neighborhood of the operating point. Nevertheless, these methods are not recommended due to the important role of the non-linear terms in describing the AUV systems. Thereupon, it is common to convert the 6-DOF model into two separate models on the horizontal and dive plane [5]. For instance, the AUV planar motion has been addressed in [6] and [7], and the depth control of AUVs has been studied in [8] and [9].

Different control methods have been applied to AUV systems for many years. A PID control for NDRE-AUV has been designed in [10], and thence, a non-linear approach has been added to the PID controller in order to improve the PID performance in [11]. In [12], a combination of genetic algorithm and PID control has been used to optimize the PID performance. In [13], a group of linear controllers have been applied to the AUV systems. Due to the inevitable presence of external disturbances in oceans and aquatic environments and inability in determining the accurate value of the hydrodynamic parameters, the robust control approaches were employed in the AUV control systems [14]. A combination of robust control and optimization algorithms have been addressed in [8] to improve the quality of control effort and in [15], particle swarm optimization algorithm was used to maximize the coverage of target area. Motivated by the aforementioned issues, the linearized model and control approaches could not be advisable in the AUV systems. Hence, the non-linear approaches seem more desirable.

The sliding mode control is regarded as a non-linear robust control together with simple implementation and common utilization in most research works on AUVs [3, 16]. However, this controller might cause the chattering phenomenon and instability in AUVs. Therefore, it tends to be combined with fuzzy, neural, and adaptive control scheme or disturbance estimator to improve its efficiency. In the fuzzy control scheme, plenty of rules are required to be adjusted, and the higher its accuracy, the greater the volume of rules and calculation time would be [17, 18], and a neural control may require an intensive calculation for learning and adaptation. Although adaptive control has been shown to be more suitable for systems with slow varying parameters, the adaptive robust control could perform superiorly in the trajectory tracking control issues in the presence of uncertainty and external disturbances [4]. Estimating disturbance in non-linear systems could also play an efficient role in the chattering elimination, especially in AUV systems in which disturbance is inevitable. In [19, 20], a finite-time tracker has been designed for tracking control of chained form non-holonomic systems using the recursive terminal sliding mode control and disturbance observer.

According to the aforementioned premises, the sliding mode control in combination with the adaptive control scheme would be recommended. In [21], the parameters of the sliding mode control have been estimated using adaptive control in order to control the depth of AUVs. In [22], a controller consisting of two loops has been designed for AUVs using the sliding mode and adaptive control. This means that position was controlled in the external loop and the desired virtual speeds were designed in order to be used for speed control in the internal loop. The switching term of the control signal has been estimated using the single-layer adaptive law in order to reduce the chattering phenomenon. In [23], a control law has been designed using a high-order sliding mode and adaptive control, in which the external disturbances have been estimated using the adaptive law. Unlike the high-order sliding mode method, the proposed method in [23] has shown no chattering phenomenon in the simulation results. In [24], a global adaptive sliding surface has been introduced to overcome the chattering phenomenon in linear systems with non-linear disturbances. In [25], the position and orientation of fully actuated AUVs on the horizontal plane have been controlled using the adaptive robust finite-time tracking control to result in robustness and accurate trajectory tracking.

Since AUVs are exposed to many disturbances such as waves, wind, and ocean currents, and what happens in the ocean is difficult to predict and susceptible of sudden change, it is necessary to consider disturbances as an unknown variable in designing the tracking control law for AUV systems. Hence, based on the approach presented in [26], the main objective of this paper is to propose the adaptive robust trajectory tracking control of AUVs on the horizontal plane exposed to external bounded disturbances with unknown boundary values. To this objective, the boundary value of disturbance and its derivative are estimated using adaptive rules. As mentioned earlier, the main drawback of the sliding mode control is the chattering phenomenon, which is a result of selecting a high-gain value for the switching term of the sliding mode control in order to obtain robustness. In order to overcome this challenge, the estimated values for

disturbances are applied to the sliding mode control law presented in this paper. In this way, the amplitude of control effort will be strong and small enough to eliminate the disturbance effects and prohibit the chattering phenomenon, respectively. Unlike other adaptive sliding mode methods, presented in the literature, which comprise the switching and equivalent term, the proposed control law consists of just one control gain, which is calculated adaptively based on the sliding mode control and unknown disturbances. Moreover, the method can also overcome unstructured uncertainty, although it is not mentioned in the paper directly.

The remainder of this paper is organized as what follows. In section 2, a 3-DOF model of AUVs on the horizontal plane is presented. The dual layer adaptive sliding mode control and its stability are given in Section 3. Section 4 provides the simulation studies, which are compared with the results of finite-time tracking control (FFTC) presented in [25], and Section 5 concludes the paper.

2. Problem formulation

The planar motion of AUVs on the horizontal plane can be developed using the earth-fixed frame {E} and body-fixed frame {B}, as illustrated in figure 1. The dynamic and kinematic equations of AUVs are expressed by (1) and (2), assuming that roll, pitch, and heave motions are negligible, and buoyancy and gravitational forces have no effect on the horizontal motion [4].

$$M\dot{v}_m + C(v_m)v_m + D(v_m)v_m = \tau + \tau_E \qquad (1)$$

$$\dot{\eta} = J(\eta)v_m \qquad (2)$$

where:

$$M = \begin{bmatrix} m - X_{\dot{u}} & 0 & 0 \\ 0 & m - Y_{\dot{v}} & 0 \\ 0 & 0 & I_z - N_{\dot{r}} \end{bmatrix} \qquad (3)$$

$$C(v_m) = \begin{bmatrix} 0 & 0 & c_{13} \\ 0 & 0 & c_{23} \\ c_{31} & c_{32} & 0 \end{bmatrix} \qquad (4)$$

$$\qquad (5)$$

$$c_{23} = (m - X_{\dot{u}})u \qquad (6)$$

$$c_{31} = (m - Y_{\dot{v}})v \qquad (7)$$

$$c_{32} = -(m - X_{\dot{u}})u \qquad (8)$$

$$D(v_m) = -\begin{bmatrix} d_{11} & 0 & 0 \\ 0 & d_{22} & 0 \\ 0 & 0 & d_{33} \end{bmatrix} \qquad (9)$$

$$d_{11} = X_u + X_{u|u|}|u| \qquad (10)$$

$$d_{22} = Y_v + Y_{v|v|}|v| \qquad (11)$$

$$d_{33} = N_r + N_{r|r|}|r| \qquad (12)$$

$$J(\eta) = \begin{bmatrix} \cos\psi & -\sin\psi & 0 \\ \sin\psi & \cos\psi & 0 \\ 0 & 0 & 1 \end{bmatrix} \qquad (13)$$

where I_z, X_u, $X_{\dot{u}}$, Y_v, $Y_{\dot{v}}$, Y_r, $Y_{\dot{r}}$, N_r, $N_{\dot{r}}$, N_v, and $N_{\dot{v}}$ are the hydrodynamic parameters. Vector $\eta = [x, y, \psi]^T$ represents the position (x, y) and orientation (ψ) of AUVs. Vector $v_m = [u, v, r]^T$ denotes linear velocities (u, v) and angular velocity around z axis (r). Vector $\tau = [\tau_1, \tau_2, \tau_3]$ describes control inputs, where τ_1 and τ_2 are the control forces and τ_3 is the control torque. Parameter τ_E is an unknown bias term, assumed as disturbance in this paper.
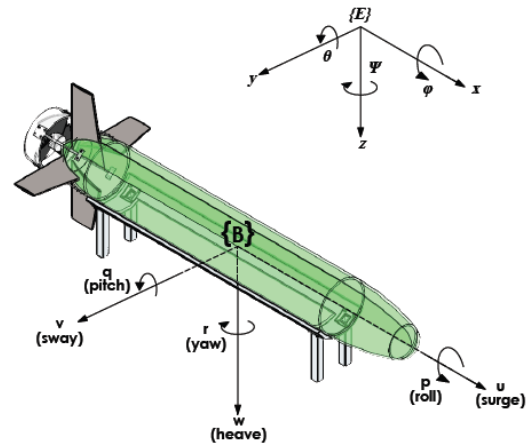

Figure 1. Earth-fixed frame and Body-fixed frame of AUVs.

3. Control design

The control objective of this paper is to design a robust control law that leads AUVs to track a desired trajectory in the presence of bounded disturbances with unknown boundary values. Dual layer adaptive and sliding mode controllers are used to achieve control objectives. First, it is essential to define the sliding surface beforehand:

$$s = \dot{e} + \alpha e \qquad (14)$$

in which $e = \eta - \eta_d$ and matrix α are a diagonal positive matrix that are determined during the design process. Equation (1) is changed to (15) by substituting v_m and its derivative, based on η, into (1) as follows [16]:

$$M_\eta(\eta)\ddot{\eta} + C_\eta(v_m,\eta)\dot{\eta} + D_\eta(v,\eta)\dot{\eta}$$
$$= \tau + \tau_E \tag{15}$$

where:

$$M_\eta(\eta) = MJ^{-1}(\eta) \tag{16}$$

$$C_\eta(v_m,\eta) = \left[C(v_m) - MJ^{-1}(\eta)\dot{J}(\eta) \right] J^{-1}(\eta) \tag{17}$$

$$D_\eta(v_m,\eta) = D(v_m)J^{-1}(\eta) \tag{18}$$

From (14),

$$\dot{\eta} = s + \dot{\eta}_d - \alpha\eta + \alpha\eta_d \tag{19}$$

$$\ddot{\eta} = s + \ddot{\eta}_d - \alpha\dot{\eta} + \alpha\dot{\eta}_d \tag{20}$$

Substituting (19) and (20) into (15) yields:

$$M_\eta(\eta)\dot{s} = -M_\eta(\eta)\ddot{\eta}_d + \alpha M_\eta(\eta)\dot{\eta}$$
$$-\alpha M_\eta\dot{\eta}_d - C_\eta(v_m,\eta)s - C_\eta(v_m,\eta)\dot{\eta}_d$$
$$+\alpha C_\eta(v_m,\eta)\eta - \alpha C_\eta(v_m,\eta)\eta_d$$
$$-D_\eta(v_m,\eta)s - D_\eta(v_m,\eta)\dot{\eta}_d \tag{21}$$
$$+\alpha D_\eta(v_m,\eta)\eta - \alpha D_\eta(v_m,\eta)\eta_d$$
$$+\tau + \tau_E$$

In order to simplify (21), the non-linear terms and disturbances are considered as an unknown term $d(t)$, which is estimated using the adaptive control scheme in the following. Hence,

$$\dot{s} = d(t) + u_c(t) \tag{22}$$

where:

$$d(t) = (\alpha\dot{\eta} - \ddot{\eta}_d - \alpha\dot{\eta}_d)$$
$$+ M_\eta^{-1}(\eta)\left(C_\eta(v_m,\eta) + D_\eta(v_m,\eta)\right)$$
$$\times (\alpha\eta - \alpha\eta_d - \dot{\eta}_d - s) \tag{23}$$
$$+ M_\eta^{-1}(\eta)\tau_E$$

$$u_c(t) = M_\eta^{-1}(\eta)\tau \tag{24}$$

Assuming that $d(t)$ and its derivative $\dot{d}(t)$ are bounded with the boundary value of d_0 and d_1, respectively, the control law is proposed [26]:

$$u_c(t) = -\left(k(t) + \beta\right)\text{sgn}\left(s(t)\right) \tag{25}$$

in which $\beta > 0$ is a small fixed design scalar and $k(t)$ is a scalar variable that is defined by the adaptation law. In order to ensure the finite time convergence to sliding manifold, the reachability condition should be satisfied:

$$s\dot{s} < -\beta|s| \tag{26}$$

Substituting (22) into (26) yields:

$$s(t)\left(d(t) + u_c(t)\right) < -\beta|s(t)| \tag{27}$$

Equation (27) can be re-written according to (25).

$$s(t)(d(t) - \left(k(t) + \beta\right)$$
$$\times \text{sgn}\left(s(t)\right) < -\beta|s(t)| \tag{28}$$

The equation given in (28) can be simplified as:

$$s(t)d(t) - k(t)|s(t)| - \beta|s(t)|$$
$$< -\beta|s(t)| \tag{29}$$

$$s(t)d(t) < k(t)|s(t)| \tag{30}$$

$$\text{sgn}\left(s(t)\right)d(t) < k(t) \tag{31}$$

from (31),

$$|d(t)| < k(t) \tag{32}$$

Hence, Equation (32) is the sufficient condition to maintain sliding surface on $s = 0$. Since during the sliding motion s is equivalent to zero, $u_c(t)$ is equal to $u_{eq}(t)$, which is the average of $u_c(t)$. As $u_{eq}(t)$ is the solution to the algebraic equation $\dot{s}(t) = 0$, when $s(t) = 0$, then according to (22) and aforementioned information:

$$u_{eq}(t) = -d(t) \tag{33}$$

Estimation of $u_{eq}(t)$ can be done by passing the signal $u_c(t)$ through a low-pass filter [27], and hence:

$$\bar{u}_{eq}(t) = \frac{1}{1 + \tau s}u(t) \tag{34}$$

$$\dot{\bar{u}}_{eq}(t) = \frac{1}{\tau}\left(-\left(k(t)+\beta\right)\mathrm{sgn}\left(s(t)\right)-\bar{u}_{eq}(t)\right) \tag{35}$$

In Equation (35), $\tau > 0$ represents a time constant, and if chosen sufficiently small, $\left|\bar{u}_{eq}(t)-u_{eq}(t)\right|$ will become small enough, and thus estimation of $u_{eq}(t)$, which is $\bar{u}_{eq}(t)$, will be more accurate. The equivalent control is employed to construct $k(t)$ by the adaptive law. Adding the safety margin and the estimated value of $u_{eq}(t)$ to condition (32) results in:

$$k(t) > \frac{1}{\mu}\left|\bar{u}_{eq}(t)\right|+\grave{o} \tag{36}$$

where $0 < \mu < 1$, and $\grave{o} > 0$ are the design scalars, which should be chosen in such a way that:

$$\frac{1}{\mu}\left|\bar{u}_{eq}(t)\right|+\frac{\grave{o}}{2} > \left|u_{eq}(t)\right| \tag{37}$$

Subsequently, the error variable is regarded as follows:

$$\delta(t) = k(t) - \frac{1}{\mu}\left|\bar{u}_{eq}(t)\right|-\grave{o} \tag{38}$$

If $\delta(t) = 0$, then:

$$k(t) = \frac{1}{\mu}\left|\bar{u}_{eq}(t)\right|+\grave{o} > \left|u_{eq}(t)\right| = \left|d(t)\right| \tag{39}$$

Consequently, the sliding mode issue can be transferred to the problem with the objective of $\delta(t) \to 0$. The $k(t)$ adaptive law is chosen as:

$$\dot{k}(t) = -\rho(t)\mathrm{sgn}\left(\delta(t)\right) \tag{40}$$

in which $\rho(t)$ is a scalar variable and symbolizes the upper bound of disturbance derivative. Its equation is assumed as:

$$\rho(t) = r_0 + r_c(t) \tag{41}$$

where $r_0 > 0$ is a constant design scalar and $r(t)$ is achieved by solving a differential equation (second layer adaptive law) in (42). Therefore, there are two adaptive laws for $k(t)$ and sc $r(t)$.

Rate of change $k(t)$ is a function of $r(t)$, which is calculated using the second layer adaptive law in (42) in such a way that it satisfies $r_0 + r(t) > \left|\dot{d}(t)\right|$, where:

$$\dot{r}_c(t) = \begin{cases} \gamma\left|\delta(t)\right| & if\ \left|\delta(t)\right| > \delta_0 \\ 0 & otherwise \end{cases} \tag{42}$$

in which $\delta_0 > 0$ is a design scalar. Besides, $e_c(t)$ is defined as:

$$e_c(t) = \frac{qd_1}{\mu} - r_c(t) \tag{43}$$

where $q > 1$ is a design safety margin scalar and

$$\left|\frac{d}{dt}(\bar{u}_{eq}(t))\right| < qd_1.$$

The block diagram of the proposed controller is shown in figure 2.

Stability condition: According to [26], the proposed control law (25) would lead to a stable sliding motion at a finite time, provided that:

- The disturbance term was considered in such a way that $\left|d(t)\right| < d_0$, and $\left|\dot{d}(t)\right| < d_1$ could be held.
- Parameters d_0 and d_1 were finite but unknown.
- Parameter $\grave{o}$ was chosen in such a way that Equation (44) was valid for any δ_0 and d_1.

$$\frac{1}{4}\grave{o}^2 > \delta_0^2 + \frac{1}{\gamma}\left(\frac{qd_1}{\mu}\right)^2 \tag{44}$$

A detailed description of the stability proof is provided in appendix A.
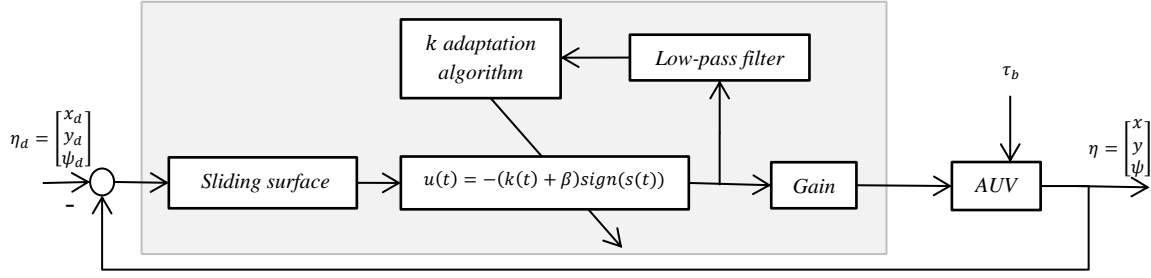
Figure 2. A block diagram of the proposed controller.

4. Simulation results

The essential hydrodynamic parameters of AUVs in the simulation studies were considered as in [4];

$m = 185\,kg$, $\quad X_u = -70\,kg/s$, $\quad X_{\dot{u}} = -30\,kg$,

$X_{u|u|} = -100\,kg/m$, $\qquad Y_v = -100\,kg/s$,

$Y_{\dot{v}} = -80\,kg$, $\quad Y_{v|v|} = -200\,kg/m$, $\quad I_z = 50\,kgm^2$,

$N_{r|r|} = -100\,kgm^2$, $\qquad N_r = -50\,kg\,m^2/s$,

$N_{\dot{r}} = -30\,kgm^2$.

Substituting these parameter values into (3-12) leads to:

$$M = \begin{bmatrix} 215 & 0 & 0 \\ 0 & 265 & 0 \\ 0 & 0 & 80 \end{bmatrix} \qquad (45)$$

$$c_{13} = -265v \qquad (46)$$

$$c_{23} = 215u \qquad (47)$$

$$c_{31} = 265v \qquad (48)$$

$$c_{32} = -215u \qquad (49)$$

$$d_{11} = -(70 + 100|u|) \qquad (50)$$

$$d_{22} = -(100 + 200|v|) \qquad (51)$$

$$d_{33} = -(50 + 100|r|) \qquad (52)$$

The initial condition of the system was assumed to be $\eta_0 = \begin{bmatrix} 0 & 110 & 0 \end{bmatrix}$. The reference trajectory described in (53-55) is a circular path with a constant velocity and an initial condition of $\eta_{d0} = \begin{bmatrix} 0 & 0 & 0 \end{bmatrix}$:

$$x_d = -100\sin(0.01t) \qquad (53)$$

$$y_d = 100\cos(0.01t) \qquad (54)$$

$$\psi_d = \arctan(\dot{y}_d / \dot{x}_d) \qquad (55)$$

The design parameters in the control strategy were $\gamma = 400$, $\dot{o} = 5$, $\delta_0 = 0.7$, $\mu = 0.99$, $\tau = 0.5$, $r_0 = 0.35$, $\alpha = diag\{2,2,2\}$, and disturbance was considered as:

$$\tau_E = \begin{bmatrix} 150\sin(0.13\pi t) \\ 150\sin(0.13\pi t) \\ 150\sin(0.13\pi t) \end{bmatrix}, \quad 200 < t < 400 \qquad (56)$$

Figures 3-8 illustrates the simulation results of the proposed controller. The results of the finite-time tracking control method [25] is presented in figures 9-12. Ultimately, to verify the effectiveness of the method, these two strategies were compared.
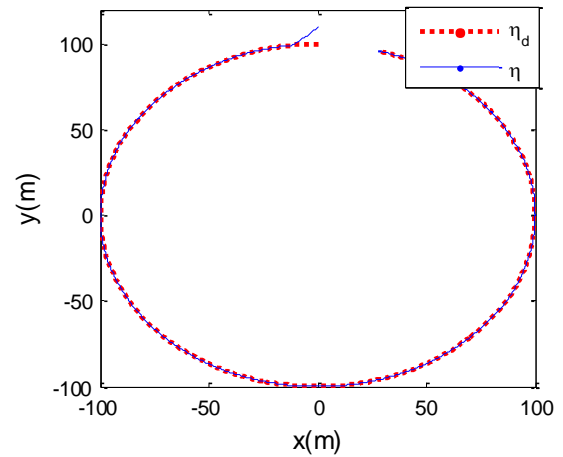

Figure 3. Trajectory tracking of AUVs using the proposed adaptive controller.

The trajectory tracking of AUVs using the pposed controller is shown in figure 3, and the tracked trajectory coincides with the desired trajectory.
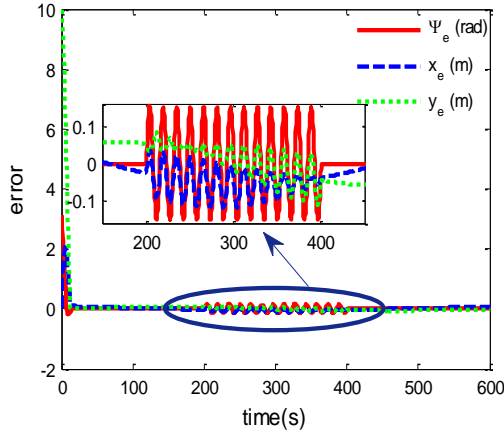
Figure 4. Position and direction errors of AUVs using the proposed controller.

Errors of position and orientation are shown in figure 4. At the beginning, because of the initial conditions and adaptation time, errors have higher values but they converge to zero in the steady-state response. At the time interval of applying the external disturbances, the error variables increase but they have small acceptable amplitudes.
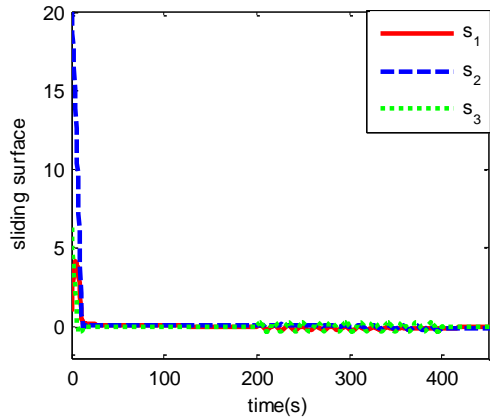

Figure 5. Sliding surfaces of the proposed controller.

The sliding surfaces of the proposed controller are shown in figure 5, and as expected, the convergence of sliding surfaces to zero can be confirmed.
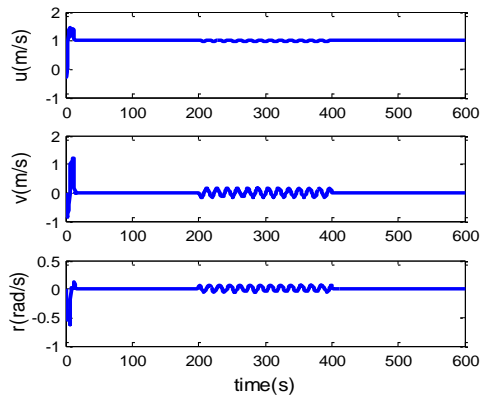

Figure 6. Linear and angular velocities of AUVs using the proposed controller.

Figure 6 depicts the linear velocities of surge and sway, and angular velocity of yaw motion. The velocities have converged constant values.
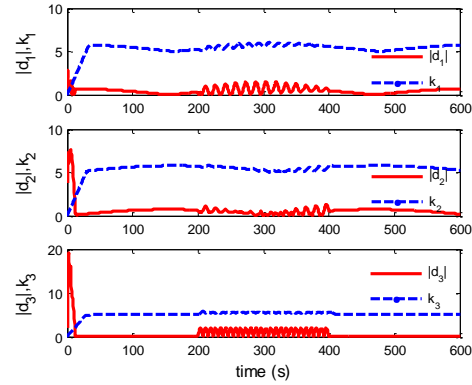

Figure 7. Gain $k(t)$ and unknown terms d(t).

The gain of the proposed controller was estimated regarding the unknown terms and external disturbances, and as it can be seen in figure 7, the estimated gain $k(t)$ satisfies $k(t) > |d(t)|$.
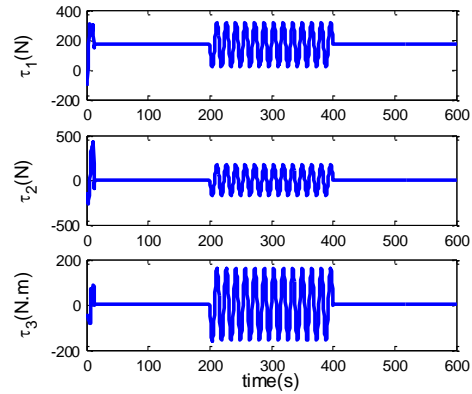

Figure 8. Control efforts of the proposed controller.

Control efforts of the proposed controller are shown in figure 8. When the external disturbances are applied to the system, the control signals vary to eliminate the disturbance effects regarding the disturbance amplitude.
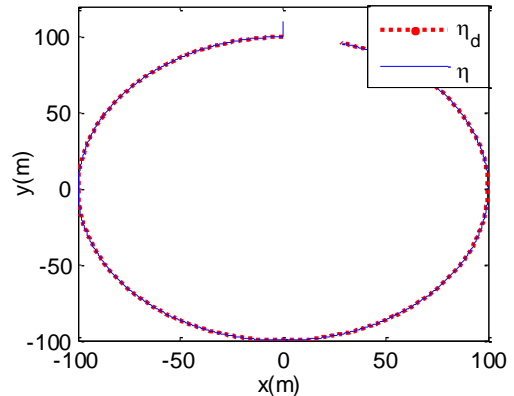

Figure 9. Trajectory tracking of AUVs using the FFTC method.

Figure 9 illustrates the desired and tracked trajectory using the finite-time tracking control presented in [25]. As it can be observed, analogous to figure 3, the tracked trajectory coincides with the desired trajectory but for a more accurate evaluation, the error figure should be assessed.
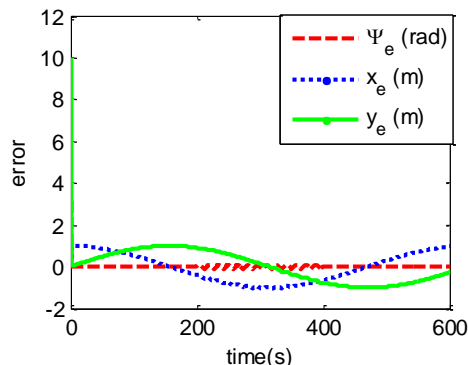

Figure 10. Position and orientation errors of AUVs using the FFTC method.

The error variables of AUV using FFTC are shown in figure 10. As it can be seen, the error amplitude is considerably larger than that in figure 4, which shows the error variables of AUVs using the proposed controller.
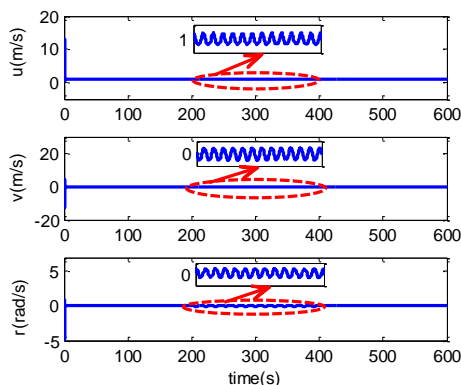

Figure 11. Linear and angular velocities of AUVs using the FFTC method.

The linear and angular velocities of AUVs using FFTC are shown in figure 11, and all velocities converge to constant values out of the disturbance interval.
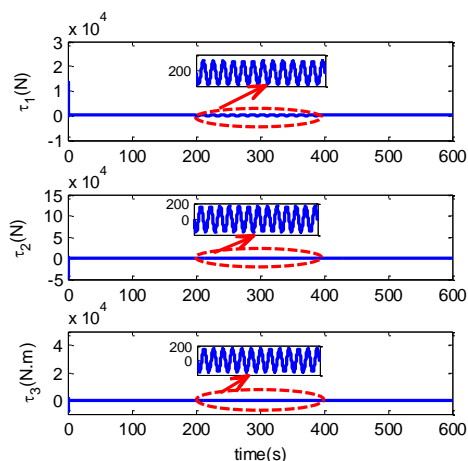

Figure 12. Control efforts of finite-time tracking control system.

The control efforts of finite-time tracking controller are shown in figure 12. Although the figure indicates no chattering in control efforts, a large initial amplitude of forces and torque in the transient response is not acceptable.

All in all, as shown in figures 3 and 9, the circular trajectory is tracked appropriately in both control applications. Although errors converge to zero in the proposed method, it oscillates with large a amplitude around zero in the FFTC scheme, which is quite observable in figure 10. Comparing the magnifications of errors in table 1, it was found that the error amplitude shows a much smaller value using a proposed controller than the FFTC method. This confirms that the proposed approach is capable of performing superiorly in the presence of defined disturbances; thus the trajectory tracking was carried out more accurately.

Table 1. Comparison of tracking errors between the proposed and FFTC methods after 30 s.

	Proposed controller			FFTC method		
	Norm	**Mean**	**Max**	**Norm**	**Mean**	**Max**
$\mathbf{x_e}$	34.8379	0.0377	0.1198	507.8712	0.6011	1.0386
$\mathbf{y_e}$	36.0943	0.0447	0.1101	559.4084	0.6876	1.0000
$\mathbf{\psi}$	47.2898	0.0336	0.1546	32.5653	0.0230	0.1030
$\mathbf{e}$	52.4064	0.0387	–	756.2615	0.4372	–

Linear velocities along x and y axes and angular velocity around z axis, employing the proposed

and FFTC method, converge to approximately constant values. Control efforts of the finite-time tracking controller, presented in figure 12, in comparison with the proposed controller in figure 8, indicates considerable large initial values. Table 2 outlines the comparison results between the proposed and FFTC methods regarding the total harmonic distortion (THD), which is a qualitative parameter indicating a measure of distortion in control signals. As it can be observed in table 2, the proposed controller performs superiorly owing to the lower values of THD, in comparison with the FFTC method.

Table 2. Comparison of Total Harmonic Distortion (THD) between the proposed and FFTC methods.

	Proposed controller (%)	FFTC method (%)
τ_1	724.19	2640.35
τ_2	408.39	3307.98
τ_3	564.11	3399.21

5. Conclusion

The main concern of this paper is the trajectory tracking control of AUVs on the horizontal plane in the presence of bounded disturbances with unknown boundary values. A two-layer adaptive control law based on the conventional sliding mode control was proposed in order to overcome the uncertainty problem.

The suggested control law not only showed robustness against system uncertainty but, unlike the conventional sliding mode controllers, the adaptive-robust method could also successfully eliminate chattering, and be designed without having information about boundary values of disturbance and its derivative, which is of great importance in AUVs operating in oceans as rare information is available about disturbances in aquatic environments. In line with the Lyapunov's second method, stability of the AUV motion in the presence of disturbances was guaranteed using the proposed controller. Ultimately, the simulation results demonstrated the adequacy and suitable performance of the proposed controller in terms of control effort and accuracy in comparison with the finite-time tracking control.

6. Recommendation

The final recommendation for future work could be employing a state observer for position estimation since it is difficult to directly measure position states in the real world.

7. Acknowledgment

References

[1] Syahroni, N., Wahyuningrat, H., Budiman, H. & Choi, J.W. (2015). Trajectory tracking for AUV with constant velocity. 2015 International Electronics Symposium (IES), Surabaya, Indonesia, pp. 85-88.

[2] Aguiar, A.P. & Hespanha, J.P. (2007). Trajectory-tracking and path-following of underactuated autonomous vehicles with parametric modeling uncertainty. IEEE Transactions on Automatic Control, vol. 52, no. 8, pp. 1362-1379.

[3] Elmokadem, T., Zribi, M. & Youcef-Toumi, K. (2016). Trajectory tracking sliding mode control of underactuated AUVs. Nonlinear Dynamics, vol. 84, no. 2, pp. 1079-1091.

[4] Xu, J., Wang, M. & Qiao, L. (2015). Dynamical sliding mode control for the trajectory tracking of underactuated unmanned underwater vehicles. Ocean Engineering, vol. 105, pp. 54-63.

[5] Rodrigues, L., Tavares, P. & de Sousa Prado, M. (1996). Sliding mode control of an AUV in the diving and steering planes. OCEANS 96 MTS/IEEE Conference Proceedings. The Coastal Ocean - Prospects for the 21st Century, Fort Lauderdale, FL, USA, 1996, pp. 576-583

[6] Repoulias, F. & Papadopoulos, E. (2007). Planar trajectory planning and tracking control design for underactuated AUVs. Ocean Engineering, vol. 34, no. 11, pp. 1650-1667.

[7] Elmokadem, T., Zribi, M. & Youcef-Toumi, K. (2017). Terminal sliding mode control for the trajectory tracking of underactuated Autonomous Underwater Vehicles. Ocean Engineering, vol. 129, pp. 613-625.

[8] Naik, M.S. & Singh, S.N. (2007). State-dependent Riccati equation-based robust dive plane control of AUV with control constraints. Ocean Engineering, vol. 34, no. 11, pp. 1711-1723.

[9] Li, J.-H. & Lee, P.-M. (2005). Design of an adaptive nonlinear controller for depth control of an autonomous underwater vehicle. Ocean Engineering, vol. 32, no. 17, pp. 2165-2181.

[10] Jalving, B. (1994). The NDRE-AUV flight control system. IEEE journal of Oceanic Engineering, vol. 19, no. 4, pp. 497-501.

[11] Perrier, M. & Canudas-De-Wit, C. (1996). Experimental comparison of PID vs. PID plus nonlinear controller for subsea robots, In: Yuh J., Ura T., Bekey G.A. (Eds), Underwater Robots. Springer, Boston, MA, pp. 121-138

[12] Chen, Q., Chen, T. & Zhang, Y. (2009). Research of GA-based PID for AUV motion control. 2009 International Conference on Mechatronics and Automation, Changchun, 2009, pp. 4446-4451.

[13] Kaminer, I., Pascoal, A., Hallberg, E. & Silvestre, C. (1998). Trajectory tracking for autonomous vehicles: An integrated approach to guidance and control. Journal of Guidance, Control, and Dynamics, vol. 21, no. 1, pp. 29-38.

[14] Feng, Z. & Allen, R. (2004). Reduced order H∞ control of an autonomous underwater vehicle. Control Engineering Practice. vol. 12, no. 12, pp. 1511-1520.

[15] Amiri, Z., Pouyan, A. & Mashayekhi, H. (2015). A topology control algorithm for autonomous underwater robots in three-dimensional space using PSO. Journal of AI and Data Mining, vol. 3, no. 2, pp. 191-201.

[16] Cheng, J., Yi, J. & Zhao, D. (2007). Design of a sliding mode controller for trajectory tracking problem of marine vessels. IET control theory & applications, vol. 1, no. 1, pp. 233-237.

[17] Zhao, S. & Yuh, J. (2005). Experimental study on advanced underwater robot control. IEEE transactions on robotics, vol. 21, no. 4, pp. 695-703.

[18] Rezazadegan, F., Shojaei, K., Sheikholeslam, F. & Chatraei, A. (2015). A novel approach to 6-DOF adaptive trajectory tracking control of an AUV in the presence of parameter uncertainties, Ocean Engineering, vol. 107, pp. 246-258.

[19] Mobayen, S. & Javadi, S. (2017). Disturbance observer and finite-time tracker design of disturbed third-order nonholonomic systems using terminal sliding mode. Journal of Vibration and Control, vol. 23, no. 2, pp. 181-189.

[20] Bayat, F., Mobayen, S. & Javadi, S. (2016). Finite-time tracking control of nth-order chained-form non-holonomic systems in the presence of disturbances. ISA transactions, vol. 63, pp. 78-83.

[21] Cristi, R., Papoulias, F.A. & Healey, A.J. (1990). Adaptive sliding mode control of autonomous underwater vehicles in the dive plane. IEEE journal of Oceanic Engineering, vol. 15, no. 3, pp. 152-160.

[22] Qiao, L. & Zhang, W. (2016). Double-loop chattering-free adaptive integral sliding mode control for underwater vehicles. OCEANS 2016-Shanghai, Shanghai, 2016, pp. 1-6.

[23] Li, X. & Zhu, D. (2016). Formation control of a group of AUVs using adaptive high order sliding mode controller. OCEANS 2016-Shanghai, Shanghai, 2016, pp. 1-6

[24] Mobayen, S., and Baleanu, D. (2016). Stability analysis and controller design for the performance improvement of disturbed nonlinear systems using adaptive global sliding mode control approach. Nonlinear Dynamics, vol. 83, no. 3, pp. 1557-1565.

[25] Wang, N., Qian, C., Sun, J.-C. & Liu, Y.-C. (2016). Adaptive robust finite-time trajectory tracking control of fully actuated marine surface vehicles. IEEE Transactions on Control Systems Technology, vol. 24, no. 4, pp. 1454-1462.

[26] Edwards, C. & Shtessel, Y.B. (2016). Adaptive continuous higher order sliding mode control. Automatica, vol. 65, pp. 183-190.

[27] Utkin, V.I. & Poznyak, A.S. (2013). Adaptive sliding mode control, In: Bandyopadhyay B., Janardhanan S., Spurgeon S. (Eds) Advances in Sliding Mode Control. Lecture Notes in Control and Information Sciences, vol. 440. Springer, Berlin, Heidelberg, pp. 21-53.

[28] Slotine, J. J. E. & Weiping Li. (1991). Applied nonlinear control. vol. 199, no. 1. Englewood Cliffs, NJ: Prentice hall, pp. 123.

Appendix A

Proof of stability condition in (44) based on the Lyapunov's theory is given as what follows [22]. The Lyapunnov function candidate is considered as:

$$V = \frac{1}{2}\delta^2 + \frac{1}{2\gamma}e_c^2 \tag{A-1}$$

Differentiating (38) leads to:

$$\dot{\delta}(t) = \dot{k}(t) - \frac{1}{\mu}\dot{\bar{u}}_{eq}(t)\,\text{sgn}\left(\bar{u}_{eq}(t)\right) \tag{A-2}$$

By substituting (41) into (40), $\dot{k}(t)$ is obtained as:

$$\dot{k}(t) = -\left(r_0 + r_c(t)\right)\text{sgn}\left(\delta_c(t)\right) \tag{A-3}$$

According to (43), it can be written that:

$$r_c(t) = \frac{qd_1}{\mu} - e_c(t) \tag{A-4}$$

Substituting (A-4) into (A-3) gives:

$$\dot{k}(t) = -\left(r_0 + \frac{qd_1}{\mu} - e_c(t)\right)\text{sgn}(\delta(t)) \qquad \text{(A-5)}$$

Therefore, $\dot{\delta}(t)$ is achieved as:

$$\dot{\delta}(t) = -\left(r_0 + \frac{qd_1}{\mu} - e_c(t)\right)\text{sgn}(\delta(t))$$
$$-\frac{1}{\mu}\phi(t)\text{sgn}(\bar{u}_{eq}(t)) \qquad \text{(A-6)}$$

where $\phi(t) = \dfrac{d}{dt}(\bar{u}_{eq}(t))$ and $|\phi(t)| < qd_1$.

Differentiating (43) results in:

$$\dot{e}_c(t) = -\dot{r}_c(t) \qquad \text{(A-7)}$$

Equation (A-8) is written using (A-6).

$$\delta\dot{\delta} = \left(e_c(t) - \frac{qd_1}{\mu}\right)\delta(t)\text{sgn}(\delta(t))$$
$$-r_0\delta(t)\text{sgn}(\delta(t)) \qquad \text{(A-8)}$$
$$-\frac{1}{\mu}\delta(t)\phi(t)\text{sgn}(\bar{u}_{eq}(t))$$

It is known that:

$$\frac{1}{\mu}\phi(t) \le \frac{1}{\mu}|\phi(t)| < \frac{qd_1}{\mu} \qquad \text{(A-9)}$$

$$\delta(t) \le |\delta(t)| \qquad \text{(A-10)}$$

Equation (A-10) leads to:

$$\frac{1}{\mu}\delta(t)\phi(t)\text{sgn}(\bar{u}_{eq}(t)) < \frac{qd_1|\delta(t)|}{\mu} \qquad \text{(A-11)}$$

Equation (A-8) is re-written using (A-11).

$$\delta\dot{\delta} \le -r_0|\delta(t)| + \left(e_c(t) - \frac{qd_1}{\mu}\right)|\delta(t)|$$
$$-\frac{qd_1}{\mu}|\delta(t)| \qquad \text{(A-12)}$$

Ultimately, (A-12) is re-written as:

$$\delta\dot{\delta} \le -r_0|\delta(t)| + e_c(t)|\delta(t)| \qquad \text{(A-13)}$$

Differentiating (A-1) leads to:

$$\dot{V} = \delta(t)\dot{\delta}(t) + \frac{1}{\gamma}e_c(t)\dot{e}_c(t) \qquad \text{(A-14)}$$

From (A-13) and (A-14), it can be concluded that:

$$\dot{V} \le -r_0|\delta(t)| + e_c(t)|\delta(t)|$$
$$+\frac{1}{\gamma}e_c(t)\dot{e}_c(t) \qquad \text{(A-15)}$$

According to (42), it can be realized that $r_c(t) \ge 0$ holds for all time, assuming that $r_c(0) = 0$. Thus it can be written from (43) that:

$$e_c(t) \le \frac{qd_1}{\mu} \qquad \text{(A-16)}$$

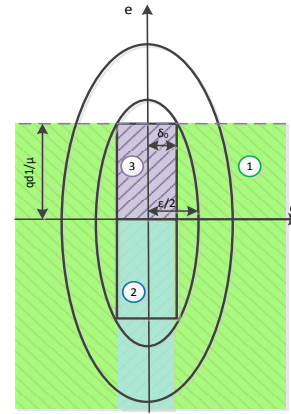Hence, stability of the indicated areas shown in "Figure 14" is only investigated.

Figure 13. Lyapunov function in term of δ and e_c.

In region 1, where $|\delta(t)| > \delta_0$ and $e_c(t) \le \dfrac{qd_1}{\mu}$, it can be written according to definition of $e_c(t)$ and $r_c(t)$ in (43) and (42):

$$\dot{e}_c(t) = -\dot{r}_c(t) = -\gamma|\delta(t)| \qquad \text{(A-17)}$$

Substituting (A-17) into (A-15) results in:

$$\dot{V} \le -r_0|\delta(t)| \qquad \text{(A-18)}$$

Thus stability of region 1 is guaranteed. In region 2, where $|\delta(t)| < \delta_0$ and $e_c(t) < 0$, substituting (42) into (A-15) results in:

$$\dot{V} \le -r_0|\delta(t)| + e_c(t)|\delta(t)| \qquad \text{(A-19)}$$

According to the assumption given for this region, i.e. e (t) < 0, it can be concluded from (A-19) that $\dot{V} \le -r_0|\delta(t)|$ stability of region 2 is also guaranteed. Region 3 is defined as:

$$F = \{(\delta, e_c): |\delta| < \delta_0, 0 \le e_c \le \frac{qd_1}{\mu}\} \qquad \text{(A-20)}$$

Consider $\bar{v}$ as the smallest ellipse centered at the origin that surrounds the rectangle of region 3, and is defined as:

$$\bar{v} = \{(\delta, e_c) : V(\delta, e_c) < \bar{r}\} \quad, \bar{r} > 0 \qquad (A\text{-}21)$$

By substituting $\left(\delta_0, \dfrac{qd_1}{\mu}\right)$ into ellipse equation, $\bar{r}$ can be obtained as:

$$\bar{r} = \frac{1}{2}\delta_0^2 + \frac{1}{2\gamma}\left(\frac{qd_1}{\mu}\right)^2 \qquad (A\text{-}22)$$

Since $F \subset \bar{v}$, and $\dot{V} \le -r_0 \left|\delta(t)\right|$ has been proved for the outside regions of ellipse, i.e. region 1 and 2, $\bar{v}$ is an invariant set. Thus if the solution $(\delta(t), e_c(t))$ enters $\bar{v}$ in finite time, then it cannot leave $\bar{v}$, and according to (44) and (A-20), $\left|\delta(t)\right| < \dfrac{\grave{o}}{2}$. Otherwise, if the solution $(\delta(t), e_c(t))$ does not enter $\bar{v}$, then $\dot{V} \le -r_0\left|\delta(t)\right|$, and:

$$\int_0^\infty \dot{V}(t)\,dt \le \int_0^\infty -r_0\left|\delta(t)\right|dt \qquad (A\text{-}23)$$

$$V(\infty) - V(0) \le -\int_0^\infty r_0\left|\delta(t)\right|dt \qquad (A\text{-}24)$$

Since the slope of the curve V is negative and V is always non-negative, its value reaches zero in infinity:

$$V(0) \ge \int_0^\infty r_0\left|\delta(t)\right|dt \qquad (A\text{-}25)$$

According to (A-25), since $V(\delta, e_c)$ is bounded for all time, $\delta(t)$ and $e_c(t)$ are bounded, and consequently, $\dot{\delta}(t)$ and $\dot{e}_c(t)$ are bounded. Thus $\delta(t)$ and $\left|\delta(t)\right|$ are uniformly continuous. Using the Barbalat's lemma [28], and (A-25), it can be written that:

$$\lim_{t \to \infty} \delta(t) \to 0 \qquad (A\text{-}26)$$

Hence, there is a finite time t_0 such that for $t > t_0$, $\left|\delta(t)\right| < \dfrac{\grave{o}}{2}$ holds. Thus regardless of whether $\delta(t)$ and $e_c(t)$ enter $\bar{v}$ or not,

$\left|\delta(t)\right| < \dfrac{\grave{o}}{2}$ is satisfied in a finite time. (A-27) can be obtained using (38).

$$\left|\delta(t)\right| = \left|k(t) - \frac{1}{\mu}\,|\bar{u}_{eq}(t)| - \grave{o}\right| < \frac{\grave{o}}{2} \qquad (A\text{-}27)$$

Therefore,

$$k(t) - \frac{1}{\mu}\,|\bar{u}_{eq}(t)| - \grave{o} > -\frac{\grave{o}}{2} \qquad (A\text{-}28)$$

and from (37),

$$k(t) > \frac{1}{\mu}\,|\bar{u}_{eq}(t)| + \frac{\grave{o}}{2} > \left|u_{eq}(t)\right| = \left|d(t)\right| \qquad (A\text{-}29)$$

According to (A-29), the condition for maintaining the sliding surface on $s = 0$ is held. Hence, stability of the controller is guaranteed.

کنترل مقاوم تطبیقی ردیابی مسیر ربات زیردریایی در صفحه‌ی افقی

نیلوفر زنده‌دل، سید جلیل ساداتی* و ابوالفضل رنجبر نوعی

گروه آموزشی برق-کنترل، دانشگاه صنعتی نوشیروانی بابل، بابل، ایران.

چکیده:

در این مقاله، کنترل ردیابی مسیر ربات زیردریایی در صفحه‌ی افقی بیان می‌شود. با فرض اینکه اغتشاش و مشتق آن کراندار با کران نامعلوم باشند، کنترل مدلغزشی تطبیقی پیشنهادی، نسبت به نامعینی‌ها و اغتشاشات امواج دریا مقاوم است. روش پیشنهادی بر اساس قانون تطبیق دولایه عمل می‌کند که بی‌نیاز از اطلاعات کران اغتشاش و مشتق آن می‌باشد. کنترل‌کننده‌ی پیشنهاد شده در این مقاله، نقش مهمی در کاهش پدیده‌ی چترینگ دارد که در کنترل‌کننده‌های مد لغزشی کلاسیک متداول است. پایداری کنترل‌کننده‌ی پیشنهادی با استفاده از تئوری لیاپانوف اثبات می‌شود و نتایج شبیه‌سازی عملکرد کنترل‌کننده‌ی پیشنهادی را نسبت به کنترل ردیابی زمان-محدود، تأیید می‌کند.

کلمات کلیدی: ربات زیردریایی، ردیابی مسیر، کنترل تطبیقی، کنترل مد لغزشی.